Glycine lithium nitrate crystals: growth and optica properties

R. González-Valenzuela, J. Hernández-Paredes, T. Medrano-Pesqueira, H.E. Esparza-Ponce, S. Jesús-Castillo, R. Rodríguez-Mijangos, V.S. Terpugov, M. E. Alvarez-Ramos and A. Duarte Möller.

Abstract

Crystals of glycine lithium nitrate with non-linear optical properties have bee grown in a solution by slow evaporation at room temperature. The crystal shows a good thermal stability from room t0emperature to 175 ◦C where the crystal begins to degrade. This property is desirable for future technological applications. Also, a good performance on the second harmonic generation was found, characterizing the emitted dominant wavelength by a customized indirect procedure using luminance and chromaticity measured data based on the CIE-1931 standard. Additionally, the 532 nm signal was detected by using a variant to the Kurtz and Perry method.

Keywords: glycine lithium nitrate; second harmonic generation; non-linear optical

Introduction

The second harmonic generation (SHG) is one of the non-linear optical (NLO) applications when the electric dipolar polarization on the material presents an interesting behavior when a high intensity light beam, such as a laser, interacts inside it. Therefore, SHG has found important applications in laser frequency modulators and also in the domain of optoelectronics and photonics. What this means is that the linear behavior of an optical material could be totally known when its electrical polarization is also linear but, increasing the power level, the polarization's equation reveals a second

degree. This effect permits a monochromatic light to travel across the material modifying its original frequency to double the value.

The crystals that promote the SHG are non-centrosymmetric and therefore piezoelectric. That is the reason why many birefringent materials also showthis effect. Here, the optical axis becomes a very important factor; when light goes parallel to this axis, both refractive indexes are equal and promote a constructive interference between the two transmitted beams (*1, 2*).

Many materials that show this effect have been found, such as amino acids that are interesting materials for NLO applications. Glycine is the simplest amino acid and published works have reported three different polymeric crystalline forms for glycine (α, β and γ) (*2–5*). Furthermore, the effect of salts in amino acids has been studied, but not too much about inorganic salts (*6*) added to glycine. This is the goal of the present work in which glycine crystals plus the added salt lithium nitrate were grown by slow evaporation technique (*7–9*).

The material characterization performed by X-ray diffraction (XRD) was reported in order to determine some of its crystalline characteristics. The FTIR spectroscopy (*10*) was done to find the functional groups and ultra-violet–visible (UV–vis) absorption (*11, 12*) was performed to observe how intense the absorption within the visible range is. Thermogravimetric analysis (TGA)/differential thermal analysis (DTA) (*13*) was also done to determine the degradation temperature, looking for high intensity application opportunities. The SHG intensity of the crystals using a variant to the powder technique was developed by Kurtz and Perry (*14*).

Experimental details

The glycine lithium nitrate (GLiN) crystals were grown in a aqueous solution by slow evaporation technique. Equimolar amount of glycine (NH3CH2COOH) and lithium nitrate ($LiNO_3$) was dissolved in double-distilled water (about 20 ml) at room temperature for about 10 min. The samples were placed at the same atmosphere on separate Petri dishes, allowing them to evaporate at a slow rate (*15*). When glycine is dissolved in water, the reaction is

$$NH_3CH_2COOH + H_2O \rightarrow (NH_2CH_2–COOH)^+$$

In this step, the molecule is ready to react with the $LiNO_3$ salt as follows:

$$NH_2CH_2{-}COOH + LiNO_3 \rightarrow C_2H_5LiN_2O_5$$

In this case, the Li^+ cations are tetrahedrally surrounded by four oxygen atoms. Three are from the glycine molecule and the fourth is from the nitrate ion.

Two more samples of pure glycine and pure lithium nitrate were also grown by the same method in order to compare them with the GLiN crystal under characterization. The sample took between 15 and 30 days to crystallize, resulting in the formation of big crystals (several millimeters in length).

Once the water evaporation was completed, the crystals were prepared for characterization with FTIR and UV–Vis spectroscopy, XRD, TGA–DTA and SHG.

Results and discussion

Optical microscopy

Before any characterization, all the samples were observed optically on the microscope before grinding. Optical Stereo Microscope Olympus Model Vanox equipment was used.

Figure 1 shows the crystal formation. Crystal sizes of 1mm length in any direction could be observed. The crystal shape showed an extended formation similar to the ones reported with different chemical compounds (*16*) and also the sharp edges with particular angles can be seen in other publications (*17*).

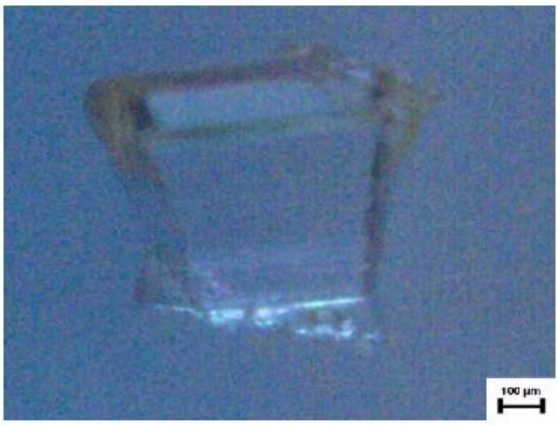

Figure 1. Glycine lithium nitrate crystal.

FTIR spectroscopy

In order to analyze the presence of functional groups, a FTIR spectrum was recorded in the range of 400–4000 cm^{-1} by using a MAGNO IR 750 series II NICOLET spectrometer. The samples were added to a matrix of KBr to perform this procedure.

Figure 2 shows the FTIR spectrum of GLiN. Additionally, on the same chart, samples of pure glycine and pure lithium nitrate are shown. The presence of the carboxyl acid group around 3000 cm^{-1} can be observed due to the presence of glycine. Then, the main internal vibrations of glycine are observed on the functional groups (NH_3^+, CH_2, COO^-) and this is in agreement with the data reported before, observing asymmetric vibrations on the NH3 and CH2 groups at 3078 and 3016 cm^{-1}, respectively.

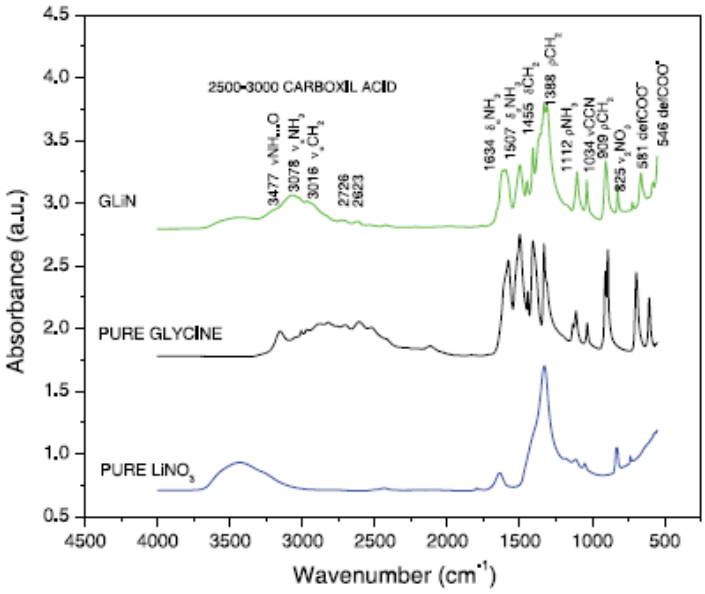

Figure 2. FTIR spectra of glycine, lithium nitrate and glycine lithium nitrate.

The peak on 892 cm−1 is a symmetrical stretching CCN. Also, the 1112 and 1132 cm^{-1} peaks are attributed to the rocking deformation of the NH_3^+ group (*11*). Furthermore, the peak at 1034 cm^{-1} is a symmetrical stretching of the CCN group. The peak 909 cm^{-1} is the rocking deformation CH_2 (*2–4*). All of these correspond to the groups observed in glycine crystals (*4, 7, 11*).

The GLiN crystal presents particular vibrations at 1043 cm−1 corresponding to the CCN group. Also, the peak at 1388 cm^{-1} is due to the COO^- bending vibration (11).

On the other hand, the peak at 837 cm^{-1} that is assigned to the C–H bending vibration and the peak at 3417 cm^{-1} corresponding to the asymmetric and symmetric OH stretching were identified (9). Other low-frequency bands are typical OF N–H · · ·O hydrogen bonds arising from the overtones around 2000 cm^{-1}. The rest of the functional groups COO^-, CN and NO_3 between 500 and 1500 cm^{-1} also agree with the reported data (2–5). Other important functional groups are detailed in Table 1.

UV–vis spectroscopy

NLO materials have a practical use only if they present a wide transparency state. To find this absorbance window, a Lambda 10 Perkin Elmer UV–Vis spectrometer was used. The scanning was done in the range of 200–1100 nm. Similar to the FTIR characterization, Figure 3 shows the UV–Vis spectrum of the GLiN plus the samples containing pure glycine and pure lithium nitrate.

An absorbance zone behind 250 nm (ultra violet wavelength) can be observed, showing a wide band completely clear in all the visible range and even more (infrared wavelengths) (2, 3, 8). This means that this material presents a good non-absorbance band inside the visible range according to the desired situation due to the expected applications. It is important to observe a little protuberance around 300 nm (4). However, this little peak is still outside the visible zone (UV zone), and it could present some absorbance if the crystal would be excited with 600 nm (red color) trying to obtain a second harmonic of 300 nm (UV color). Other noticeable characteristic in the absorption spectra is a wide transparency window within the range of 400–1100 nm, which is desirable for NLO crystals because the absorptions in an NLO material near the fundamental or second harmonic signals will lead to the loss of the conversion of SHG. Due to this property, GLiN has potential uses for SHG using a Nd:YAG laser (1064 nm) to emit a second harmonic signal within the green region (532 nm) of the electromagnetic spectrum. But GLiN is not a candidate for the third (355 nm) or fourth (266 nm) harmonics of Nd:YAG.

Table 1. Functional groups of glycine lithium nitrate.

cm^{-1}	Gly:$LiNO_3$	cm^{-1}	Gly:$LiNO_3$
3417	$\nu_{as}OH$	1388	$\nu_s COO^-$
3078	$\nu_a NH_3$	1132	ρNH_3
3016	$\nu_a CH_2$	1112	ρNH_3
2726	Overtone	1034	νCCN
2623	Overtone	909	ρCH_2
2537	Overtone	892	νCCN
2422	Overtone	837	$\nu C–H$
2007	Overtone	825	$\nu_2 NO_3$
1757	Overtone	722	$\nu_4 NO_3$
1634	$d_a NH_3$	667	$dCOO^-$
1507	$d_s NH_3$	581	$defCOO^-$
1455	dCH_2	546	$defCOO^-$

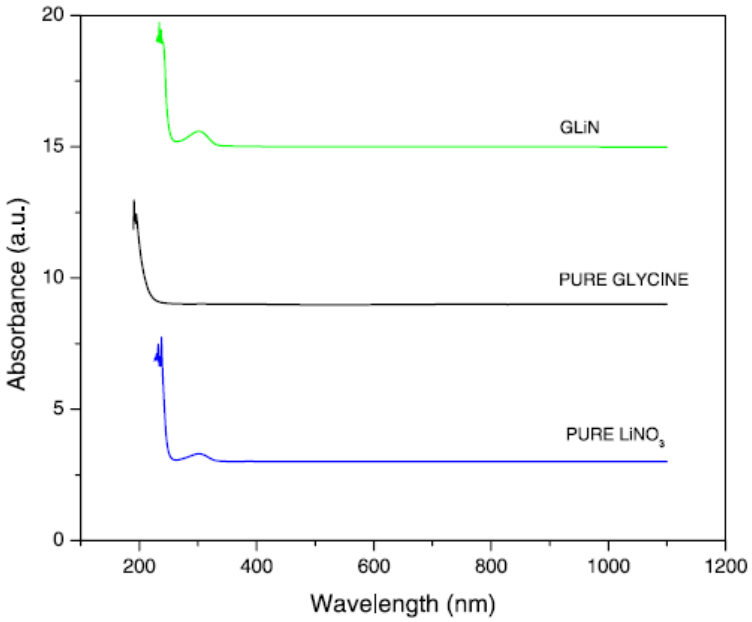

Figure 3. UV–vis spectra of glycine, lithium nitrate and glycine lithium nitrate.

X- ray diffraction

The XRD data were collected using a X-PERT Phillips diffractometer with CuKα (λ = 1.540598Å), step of 0.05° and 2θ scanning between 10° and 60°. Finally, the samples were powders of crystals.

Like other characterizations, GLiN, pure glycine and pure lithium nitrate are shown together. Figure 4 shows the XRD pattern. Within the graph appear the main peaks taken from database information of the α-glycine, that is, a monoclinic crystal with lattice parameters (a = 5.4621Å, b = 11.966Å, c = 5.1077Å) and spatial group P21/*n*. This crystal structure and spatial group are found in the L-argininum dinitrate (*13*) and lithium p-nitrophenolate (*16*).

In the same way, the database information for lithium nitrate was found, observing a hydrated phase in an orthorhombic system (17) with lattice parameters (a = 6.803Å, b = 12.718Å, c = 6.002Å) and spatial group Cmcm. Table 2 displays the corresponding information for both α-glycine and hydrated lithium nitrate. A non-centrosymmetric structure was expected to be obtained for GLiN. The options to have this kind of symmetry are the crystal systems triclinic, monoclinic and orthorhombic. Two of them can be shown on the crystals with single glycine and lithium nitrate with good agreement with the literature.

Thermogravimetric analysis/differential thermal analysis

TGA/DTA was done in a TA Instruments STD 2960 Simultaneous DTA–TGA. The samples were heated from room temperature to more than 1000◦C at a rate of 10°C/min.

The TGA spectra of GLiN, pure glycine and pure lithium nitrate displayed in Figure 5 shows that GLiN and pure glycine present similar behavior with a little

difference from the pure lithium nitrate sample, showing a good stability below 250 ◦C with a rapid dropping beyond that temperature (2, 7).

Figure 6 presents the DTA spectra of GLiN, pure glycine and pure lithium nitrate. GLiN presents an endothermic transition around 175 °C and an exothermic one at about 250 °C. Meanwhile, the pure glycine and lithium nitrate samples show a important endothermic transitions at 250 °C. LiNO3 shows another endothermic transition at 600°C (2, 7).

Within this temperature range, the possible NLO applications become promising, due to the use of laser powers, showing a good performance below 250 °C.

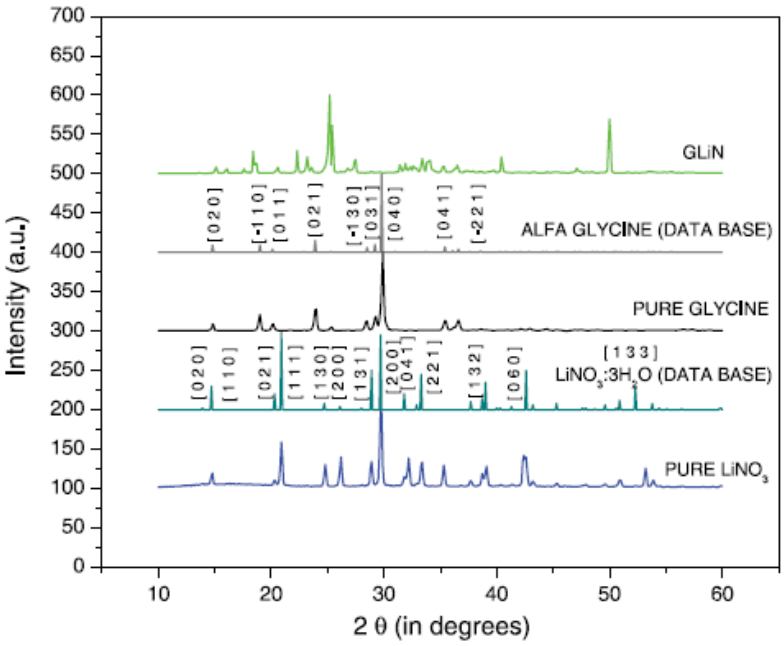

Figure 4. XRD pattern of glycine lithium nitrate.

Table 2. Spatial groups and reticular parameters of α-glycine and $LiNO_3.3H_2O$.

$2F$	α-Glycine (h k l)	$LiNO_3.3H_2O$ (h k l)
13.913		0 2 0
14.752		1 1 0
14.802	0 2 0	
18.988	−1 1 0	
20.119	0 1 1	
20.352		0 2 1
20.935		1 1 1
23.908	0 2 1	
24.724		1 3 0
26.181		2 0 0
28.457	−1 3 0	
28.909		1 3 1
29.228	0 3 1	
29.777		2 2 0
29.858	0 4 0	
31.843		0 4 1
33.369		2 2 1
35.423	0 4 1	
36.604	−2 2 1	
39.081		1 3 2
42.612		0 6 0
52.294		1 3 3
System	Monoclinic	Orthorombic
Spatial group	P21/n (14)	Cmcm (63)
a	5.4621	6.803
b	11.966	12.718
c	5.1077	6.002
Alfa	90	90
Beta	111.72	90
Gamma	90	90
Z	4	4

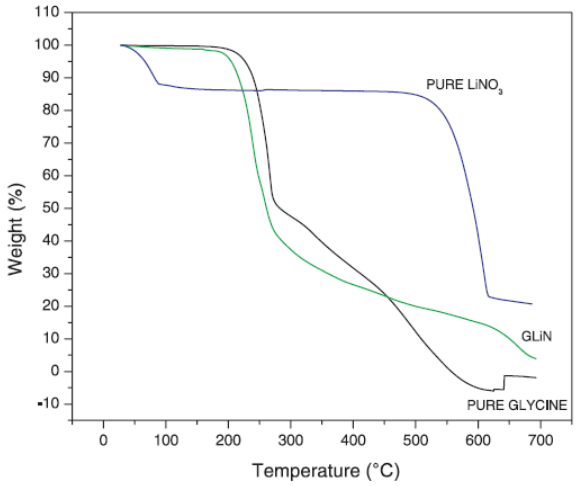

Figure 5. TGA spectra of glycine lithium nitrate.

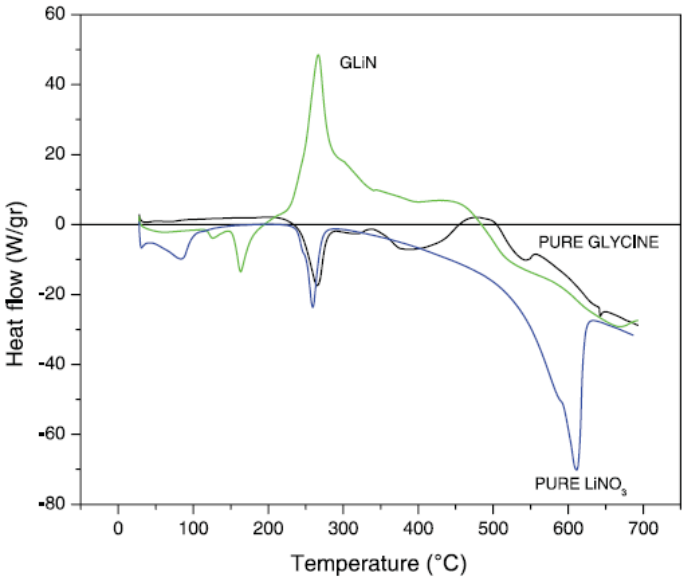

Figure 6. DTA spectra of glycine lithium nitrate.

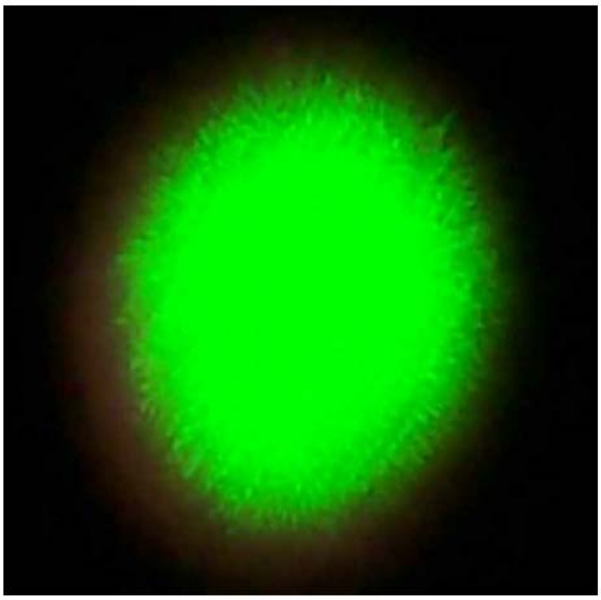

Figure 7. Image of transmitted SHG of glycine lithium nitrate.

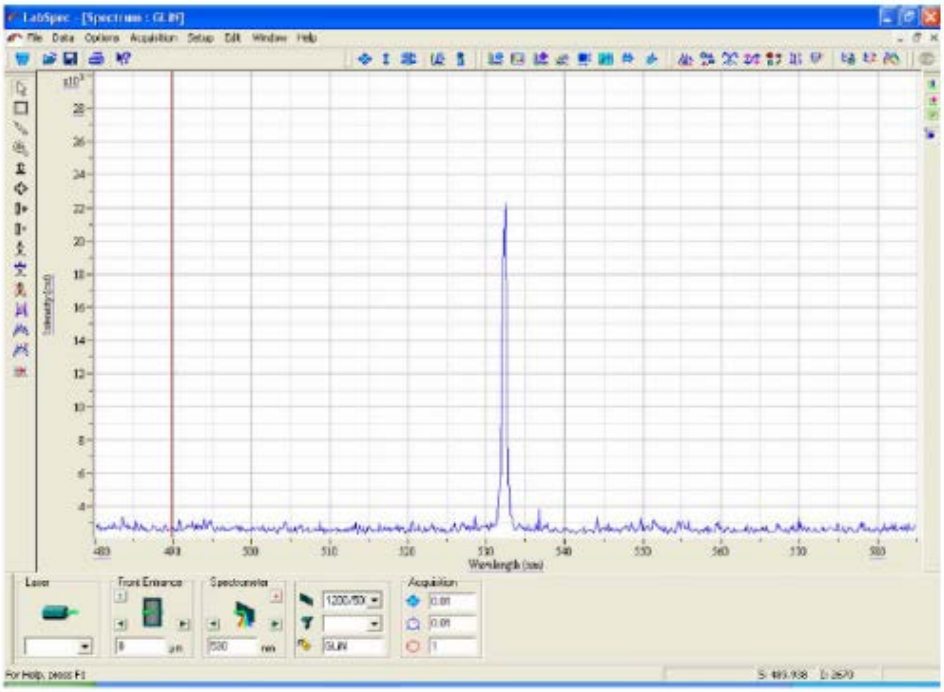

Figure 8. Spectral emission of SHG of glycine lithium nitrate. The maximum is located at 532 nm.

SHG measurement

In order to find the SHG, the crystals were ground by using a variant to the Kurtz and Perry technique into powder (about 70μm) and densely packed between two transparent microscope glass slides (15, 17).

Once the samples are placed on the glass slides, a Nd:YAG Quanta ray INDI series laser of 1064 nm, generating an 8 ns pulse and operating at 6mJ/pulse and at a rate of 10 Hz, is pumped at the proper angle and distance in order to see visibly the SHG in the green color region (532 nm), the expected emitted half wavelength signal.

Afterwards, the green emitted lightwas photographed in order to evidence the double-frequency emission or SHG shown in Figure 7. As a quantitative measurement of the green light emitted by the crystal, Figure 8 displays the emission spectra where the peak located at an wavelength of 532 nm is clearly noticeable, exactly the half of the incident radiation come in from a Nd-YAG laser (1064 nm). This SHG signal was detected by using a JobinYbon ICCD model Spectrum Two attached in a Jobin Ybon

Triax-550 monochromator. Because a variant to the Kurtz and Perry method has been used, where a reference beam and standard sample was not used, it was not possible to quantify the quantum efficiency with respect to a standard NLO single crystal such as KDP or urea. However, it is the future challenge for this research.

Conclusions

Good quality crystals of GLiN were grown by slow evaporation technique, verifying its main functional groups by FTIR and comparing them with reported data. Also, based on UV–Vis spectra observations, an absorption zone under 250 nm (ultra-violet wavelengths) can be seen, recovering a good transmittance values across all the visible range until near IR frequencies and beyond. This situation gives us the confidence of applying this crystal for applications involving the band of visible light.

Other characterization was the thermal response. There, the TGA/DTA results degrading temperature of about 250 °C, which promises to have good applications at high temperatures, revealing that the crystal is thermally stable until that temperature.

Finally, an evidence of the second harmonic generation property of GLiN has been detected and shown by using a modification to the Kurtz and Perry method.

Acknowledgements

The authors thank Daniel Lardizabal from CIMAV, México, for his technical help. Ricardo González gratefully acknowledges his doctoral fellowship provided by the National Council of Science and Technology, CONACYT, México. Thiswork was partially supported by Consejo Nacional de Ciencia y Tecnología (CONACYT), México, under project 2008-90533 and PROMEP under project P/CA-121 2006-26-20.

References

(1) Hetch, E.; Zajac, A. Optics; AddisonWesley: Reading, England, 1974.

(2) Narayan Bhat, M.; Dharmaprakash, S.M. J. Cryst. Growth 2002, 236, 376–380.

(3) Ambujam, K.; Rajarajan, K.; Selvakumar, S.;, Vetha, I.;, Ginson, P.; Sagayaraj, P. J. Cryst. Growth 2006, 286, 440–444.

(4) Narayan Bhat, M.; Dharmaprakash, S.M. J. Cryst. Growth 2002, 235, 511–516.

(5) Narayan Bhat, M.; Dharmaprakash, S.M. J. Cryst. Growth 2002, 242, 245–252.

(6) Kamiyama, T.;Miyamoto, A.; Kawamura, J.; Nakamura,Y.; Kiyanagi,Y. J. Phys. Chem. Solids 1999, 60, 1549–1552.

(7) Selvaraju, K.; Valluvan, R.; Kumararaman, S. Mater. Lett. 2006, 60, 2848–2850.

(8) Lakshmanaperumal, C.K.; Arulchakkaravarthi, A.; Balamurugan, N.; Santhanaraghavan, P.; Ramasamy, P. J. Cryst. Growth 2004, 265, 260–265.

(9) Boaz, B.M.; Rajesh, A.L., Jesu, S.X.; Das, S.J. J. Cryst. Growth 2004, 262, 531 535.

(10) Markarian, S.A.; Gabrielian, L.S.; Zatikyan, A.L.; Bonora, S.; Trinchero, A. Vib. Spectr. 2005, 39, 220–228.

(11) Shanmugavadivu, Ra.; Ravi, G.; Nixon Azariah, A. J. Phys. Chem. Solids 2006, 67, 1858–1861.

(12) Madhavan, J.; Aruna, S.; Prabha, K.; Packium, J.; Ginson, J.; Joseph, P.; Selvakumar, S.; Sagayaraj, P. J. Cryst. Growth 2006, 293, 409–414.

(13) Thomas, C.; Thomas, J.; Packiam, J.; Madhavan, J.; Selvakumar, S.; Sagayaraj, P. J. Cryst. Growth 2005, 277, 303–307.

(14) Kurtz, S.K.; Perry, T.T. J. Appl. Phys. 1968, 39, 3798–3813.

(15) Narayana Moolya, B.; Jayarama,A.; Sureshkumar,M.R.; Dharmaprakash, S.M. J. Cryst. Growth 2005, 280, 581–586.

(16) Boaz, B.M.; Das, S.J. J. Cryst. Growth 2005, 279, 383–389.

(17) Selvaraju, K.; Valluvan, R.; Kumararaman, S. Mater. Lett. 2006, 60, 2848–2850.